



HAL
open science

Categorization of neural excitability using threshold models

Arnaud Tonnelier

► **To cite this version:**

Arnaud Tonnelier. Categorization of neural excitability using threshold models. *Neural Computation*, 2005, 17 (7), pp.1447-1455. inria-00000581v2

HAL Id: inria-00000581

<https://hal.science/inria-00000581v2>

Submitted on 3 Jun 2009

HAL is a multi-disciplinary open access archive for the deposit and dissemination of scientific research documents, whether they are published or not. The documents may come from teaching and research institutions in France or abroad, or from public or private research centers.

L'archive ouverte pluridisciplinaire **HAL**, est destinée au dépôt et à la diffusion de documents scientifiques de niveau recherche, publiés ou non, émanant des établissements d'enseignement et de recherche français ou étrangers, des laboratoires publics ou privés.

Categorization of Neural Excitability using Threshold Models

A. Tonnelier

Cortex Project, INRIA Lorraine, Campus Scientifique, B.P. 239, 54 506

Vandoeuvre-lès-Nancy, France

Abstract

A classification of spiking neurons according to the transition from quiescence to periodic firing of action potentials is commonly used. Nonbursting neurons are classified into two types, type I and type II excitability. We use simple phenomenological spiking neuron models to derive a criterion for the determination of the neural excitability based on the afterpotential following a spike. The crucial characteristic is the existence for type II model of a positive overshoot, i.e. a delayed afterdepolarization, during the recovery process of the membrane potential. Our prediction is numerically tested using well known type I and type II models including the Connor *et al.* model and the Hodgkin-Huxley model.

1 Introduction

Despite the large number of ionic mechanisms underlying the initiation of action potentials, a broad class of non-bursting neurons presents two types of excitability (Hodgkin, 1948; Rinzel & Ermentrout, 1998; Izhikevich, 2000). The properties of membrane excitability are determined according to the emerging

frequency of repetitive firing. Type I is obtained when repetitive action potentials are generated with an arbitrarily low frequency, whereas in type II spike trains emerge at a nonzero frequency. The frequency response of a single cell is crucial since it models the input-output relation, i.e. the gain function, commonly used in firing rate description of neural networks. The dynamics of the membrane excitability determines the spike train statistics (Gutkin & Ermentrout, 1998) and is fundamental to understand how non-trivial dynamics emerge when neurons are coupled in networks (Hansel *et al.*, 1995).

Previous works on the classification of excitability used the bifurcation theory (Ermentrout, 1996; Rinzel & Ermentrout, 1998; Izhikevich, 2000). The bifurcation resulting in the apparition of a stable limit cycle determines the type of excitability. Typically, type I and II are related to a saddle node bifurcation on an invariant circle and an Andronov-Hopf bifurcation, respectively. However this classification is not perfect and one has to distinguish between the bifurcation of the resting state and the bifurcation of the limit cycle leading to a complex classification (Izhikevich, 2000).

The purpose of the manuscript is to derive a simple criterion for the classification of neural excitability. In an earlier paper (Tonnelier & Gerstner, 2003) the authors showed that type I and type II neurons can be obtained as a generalization of integrate-and-fire neurons. However, the question of the classification based on the firing rate was not addressed and the neural mechanisms that distinguish between the two types of excitability was not established. In this note, we present an easy and intuitive way to characterize the neural excitability of spiking neurons using the analytical framework of the spike-response model. The result is surprisingly simple: type I is obtained when the afterpotential

following a spike has a monotonic recovery process whereas type II membranes present a small depolarization during the recovery. We check the validity of this classification on more complex models and derive some qualitative and quantitative predictions.

2 Type I vs. Type II Excitability of the Spike-Response Model

The spike-response model allows for a phenomenological description of spiking neurons (Gerstner & Kistler, 2002). This model approximates the dynamics of biophysical detailed models with a great accuracy (Kistler *et al.*, 1997; Jolivet *et al.*, 2004) and yields to a transparent discussion of various neural dynamics (Gerstner *et al.*, 1996). In this model, the membrane potential $v(t)$ in response to a constant stimulation is given by

$$v(t) = \sum_{t^f \in \mathcal{F}} \eta(t - t^f) + u_{\text{stat}}(I)$$

where $\eta(t - t^f)$ describes the form of a spike and the afterpotential following it. The second term $u_{\text{stat}}(I)$ models the response of the membrane potential to a constant input current I , i.e. the steady-state $I - V$ relationship of the model (to simplify the notations, we will drop the dependence on I). It is convenient (Tonnelier & Gerstner, 2003) to split the kernel η into two parts

$$\eta(t - t^f) = \eta_f(t - t^f) - \eta_r(t - t^r)$$

where η_f and η_r are two pulse-shaped kernels. The first term η_f describes the spike, i.e. the abrupt depolarization of the membrane potential, and $-\eta_r$ models the recovery period that follows the spike, i.e. the spike-afterpotential.

The action potential is triggered at time $t = t^f \in \mathcal{F}$ where the set \mathcal{F} gives the spike events that are to be taken into account. A spike event occurs if the membrane potential crosses a threshold ϑ from below. The recovery kernel acts at the so-called resetting time $t^r = t^f + \Delta$ where Δ includes the spike duration and an absolute refractory period. The kernel η_f operates on a fast time scale and we approximate it by a Dirac delta function. Since the membrane trajectory during a spike reflects the membrane properties and not the input, the kernel η_r is independent of the input.

To reproduce the recovery processes of neurons, we consider the two following kernels

$$\eta_r^I(t) = \mu_r e^{-t/\tau_r} \sinh \omega_r t, \quad (1)$$

$$\eta_r^{II}(t) = \mu_r e^{-t/\tau_r} \sin \omega_r t, \quad (2)$$

for $t > 0$ and 0 otherwise, that we call type I and type II recovery kernels, respectively. The parameter μ_r is a scale factor, τ_r is the recovery time constant and ω_r determines the global shape of the kernel. We require $\omega_r \tau_r < 1$ for type I recovery kernel in order to ensure a decay to 0. Note that these two kernels could be written in a general formalism using complex values of ω_r .

We will show the following result : type I and type II recovery kernels describe type I and type II membrane models, respectively. The existence for type II kernel of a negative part, i.e. a positive overshoot of the corresponding membrane potential, is the main difference between the two kernels. The precise form of η_r is not important; a similar result holds for different choices.

2.1 Analytical treatment

A constant input current generates an indefinite train of spikes if $t^f = n/\nu$ where n is the index of the n^{th} spike and ν is the mean firing rate. We note $v_\infty(t)$ the membrane potential in the repetitive spiking regime. For clarity, we take, in our analytical treatment, $\Delta = 0$. We calculate

$$v_\infty(t) = \sum_n \delta(t - n/\nu) - \eta_{r,\infty}(t) + u_{\text{stat}} \quad (3)$$

where $\eta_{r,\infty}$ is the periodic recovery kernel that we calculate using summation formula. We find

$$\eta_{r,\infty}^I(t) = \frac{\mu_r}{2(\cosh T/\tau_r - \cosh \omega_r T)} \left(e^{\frac{T-t}{\tau_r}} \sinh \omega_r t + e^{-\frac{t}{\tau_r}} \sinh \omega_r (T-t) \right)$$

and

$$\eta_{r,\infty}^{II}(t) = \frac{\mu_r}{2(\cosh T/\tau_r - \cos \omega_r T)} \left(e^{\frac{T-t}{\tau_r}} \sin \omega_r t + e^{-\frac{t}{\tau_r}} \sin \omega_r (T-t) \right)$$

for $0 \leq t \leq T$ where $T = 1/\nu$ is the interspike interval. The frequency of the periodic firing is obtained from the requirement $v_\infty(T) = \vartheta$ that we rewrite $F(x) = \vartheta_e$ where $x = \omega_r \nu^{-1}$,

$$F^I(x) = \frac{\sinh x}{2(\cosh x - \cosh \alpha x)}, \quad (4)$$

$$F^{II}(x) = \frac{\sin x}{2(\cos x - \cosh \alpha x)}, \quad (5)$$

ϑ_e is the effective dimensionless threshold defined by $\vartheta_e = (\vartheta - u_{\text{stat}})/\mu_r$ and $\alpha = 1/\omega_r \tau_r$. For type II kernel, α is the ratio between its oscillatory period and its decaying time constant. Type I kernel could be expressed as a difference between two exponentials with two time scales (a rising time τ_1 and a decaying time τ_2) and α represents $(\tau_1 + \tau_2)/(\tau_2 - \tau_1)$. In addition to (4),(5), the neuronal voltage should exceed ϑ only once during one period

$$v_\infty(t) < \vartheta, \quad t \in (0, T). \quad (6)$$

A necessary, but not sufficient, condition reads $-d\eta_{r,\infty}(T)/dt > 0$, i.e. the voltage increases just before the spike.

First, we consider the type I function (4). Using the requirement $\alpha = 1/\tau_r\omega_r > 1$ for type I kernel, it is straightforward to show that a necessary and sufficient condition for the existence of a repetitive spiking regime is $\vartheta_e < 0$, or equivalently $u_{\text{stat}} > \vartheta$, that states that the stationary potential crosses the threshold, i.e. the stationary state disappears. Note that the periodic solution is unique since F^I is monotonic increasing with respect to x . At the critical regime, $\vartheta_e \rightarrow 0$, periodic firing appears with an arbitrarily low frequency, $\nu^I \rightarrow 0$, and from (4) we derive the following logarithmic law for the emerging frequency

$$\nu^I = (\omega_r - 1/\tau_r)[\ln -2\vartheta_e]^{-1}. \quad (7)$$

Determination of the critical current is obtained giving the dependence of the stationary state u_{stat} with respect to I . For instance, if we consider the steady state $I - V$ curve of the standard IF model, we have $u_{\text{stat}} = RI$ and we find the well known critical current $I_c = \vartheta/R$ for the emergence of repetitive spiking. Note that the logarithmic law (7) of the frequency-current relationship is closely related to the exponential decrease of the recovery kernel η_r . A square-root law is obtained when considering a quadratic decay of the recovery kernel.

We now investigate the type II system: $F^{II}(x) = \vartheta_e$. Using (5), we show in Figure 1B the locus of existence of the repetitive firing regime. There exists a critical threshold $\vartheta_e^*(\alpha) > 0$ such that the existence of periodic spiking solution is obtained for $\vartheta_e < \vartheta_e^*$. Solutions appear by pair but one violates the condition (6). Periodic firing appears before the vanishing of the stationary state and a bistability regime exists for $0 < \vartheta_e < \vartheta_e^*$ where a stationary state and a peri-

odic solution coexist. Qualitatively, the explanation is based on the existence of a depolarized afterpotential that drives the membrane potential into the superthreshold regime and therefore repetitive firing appears before the vanishing of the stationary state. At the critical regime, $\vartheta_e = \vartheta_e^*$, it is clear from (5) that small values of ν (x infinite) are not solutions, i.e. periodic firing emerges with a nonzero frequency.

The exponential decay of the recovery kernel implies that the summation over the firing time is dominated by the most recent firing event. Hence, the periodic kernel $\eta_{r,\infty}$ is well approximated at time t by $\eta_r(t)$. This approximation, reported as the "short-term memory approximation" (Gerstner & Kistler, 2002), leads to an accurate determination of the emergence of repetitive firing given by $-\eta_r(\nu^{-1}) = \vartheta_e$ (see Figure 1B) and fits the exact periodic solution (see Figures 1C, 1D). In this approximation, the frequency of the emerging periodic firing for type II kernel is given by

$$\nu^{II} = [\Delta + \omega_r^{-1}(\pi + \arctan(\omega_r \tau_r))]^{-1} \quad (8)$$

In other words, the location of the delayed afterdepolarization of type II models could be used as an approximation of the period of the emerging repetitive spiking regime.

2.2 Type I vs. Type II Neural Excitability

Our analysis of the spike-response model suggests a simple observable criterion for determining the excitability of spiking neurons based on the recovery process following an action potential elicited by a brief current pulse: the afterpotential of type I models is hyperpolarized whereas type II models present a delayed afterdepolarization (DAD), also reported as a prolonged depolarized afterpoten-

tial. In this part we aim at establishing some connections with detailed models and thus deriving some quantitative predictions. In Figure 1E, 1F we look at the time-course of the action potential of popular type I and type II models. In Figure 1E we show the action potential of models reported as type I: the Connor *et al.* model and the Morris-Lecar model in the type I regime (see Ermentrout, 1996). Panel F shows the voltage trajectories of type II models : the Hodgkin-Huxley (HH) model and FitzHugh-Nagumo model. A large number of papers and books describing the equations and the dynamics of these models are available (Koch, 1999; Gerstner & Kistler, 2002). Since they represent different aspects of nerve cell excitability, these models are widely used as paradigmatic models of action potential generation.

Numerically, parameters μ_r , τ_r , ω_r , and Δ are adjusted such that the kernels (1), (2) fit the time course of the membrane afterpotential of the detailed neural models (see Figures 1E, 1F). We see that type II kernels numerically fit the afterpotential of the Hodgkin-Huxley and FitzHugh-Nagumo models whereas type I kernels approximate the afterpotential of the Connor *et al.* and Morris-Lecar models. The correspondence between the kernels and the detailed models are made near the onset of repetitive firing. Different parameter values do not affect the categorization, i.e. the type of the kernels remains unchanged, provided that we work away from the hyperexcitable regime since at highly depolarized potentials both type I and type II models can show afterdepolarization.

Let us now numerically illustrate some quantitative predictions. We mainly examine the Hodgkin-Huxley (HH) model but a similar analysis can be carried out for the other models. Parameters for the recovery kernel of the HH model are given in Figure 1. Using (5), i.e. solving $F^{II}(x) = \vartheta_e$, we find an emerging

frequency $\nu^{II} = 51Hz$ and using (8) we find the approximate value $52Hz$. These results fit the exact value of the complete model (about $53Hz$ at $6.3^\circ C$). To go further, i.e to find the critical current, one needs to elucidate (i) the steady state $I - V$ relationship and (ii) the threshold behavior. Despite the nonlinearity of the full model, the steady-state membrane depolarization in the subthreshold regime depends linearly on the applied membrane current (Koch, 1999). The numerical fit (simulations not shown) of the steady-state $I - V$ curve is given by

$$u_{\text{stat}} = u_0 + RI \text{ where } u_0 = -65.0 \text{ mV}, R = 0.7M\Omega \text{ cm}^2 \quad (9)$$

for $u_{\text{stat}} < \vartheta$ (the stable branch of the $I - V$ curve for the Connor model is also well fitted with (9) using $u_0 = -68mV$). It has been observed that the Hodgkin-Huxley equations exhibit a threshold behavior (Koch, 1999; Gerstner & Kisler, 2002). For the extraction of the threshold, we used a rapid and strong input current, i.e. a certain amount of electrical charge is instantaneously delivered to the membrane, and we find a voltage threshold for spike initiation given by $\vartheta = -58.2mV$ (see also Noble & Stein, 1966). Then, we predict that the stationary state destabilizes at $I = 9.4\mu A/cm^2$ (using $u_{\text{stat}} = \vartheta$) whereas the critical current of emerging repetitive firing is given by $I_c = 6.6\mu A/cm^2$ (using (5)) and $I_c = 5.9\mu A/cm^2$ in the short memory approximation. Our result emphasizes the difference between voltage-threshold and current-threshold (Koch *et al*, 1995). If we define the current-threshold, also referred as the rheobase, as the critical value of a sustained current initiating action potentials, type II model leads to a corresponding membrane potential (given by the steady-state $I - V$ curve) below the voltage-threshold ϑ whereas these two thresholds coincide for type I models.

3 Discussion

One possible classification of neurons uses the discontinuity of the firing rate curve. Following this categorization and in the framework of the spike-response model, we have shown that type I and type II recovery kernels account for the difference between type I and type II spiking models. Regarding this result, we state that the spike afterpotential could be used as a characteristic of membrane excitability. Our approach has some connections with the classification based on the bifurcation theory. Indeed, the oscillations generated by the Hopf bifurcation produce a DAD that leads to the type II response predicted by the bifurcation theory and by our criterion. However, we stress that the existence of a DAD does not require the existence of subthreshold oscillations. In fact, damped oscillations are related to the bifurcation of the resting state that can be different from the bifurcation of the limit cycle as it is the case when bistability occurs, i.e. the coexistence of a stable limit cycle and a stable resting state. The existence of the DAD is related to the limit cycle bifurcation.

Our approach is highly simplified and neglects many aspect of neuronal dynamics. We used a threshold for spike-initiation and we neglected the other nonlinear processes for the generation of spikes. However, our result could be used as a criterion for the classification of neural excitability of detailed models away from their hyperexcitable regime. In conductance-based models, the depolarized spike-afterpotential appears because of an interplay between the subthreshold voltage-gated currents. The membrane potential during this stage is mainly driven by the dynamics of potassium current(s). Therefore, we suggest that the type I or type II excitability is mainly determined by the voltage-dependent potassium current(s). This intuition is corroborated by the transition

between type I and type II excitability when changing the potassium dynamics of the Morris-Lecar model (Rinzel & Ermentrout, 1998). More precisely, it can be shown that the transition from type I to type II Morris-Lecar model can be monitored only by changing the potassium activation curve. Therefore, as suggested by our analysis, the neural excitability of the Morris-Lecar model could be characterized observing its spike recovery. Note also that the main difference between the Hodgkin-Huxley model and the Connor *et al.* model is the existence of an additional A-type potassium current leading to a type I response in the Connor *et al.* model. We stress that other mechanisms can be put forward to explain excitability changes, such as the existence of a transient calcium conductance, but the potassium currents are probably the most commonly encountered mechanism that determines the neural excitability.

Acknowledgments The author thanks Wulfram Gerstner for valuable suggestions.

References

- Ermentrout, G.B. (1996). Type I membranes, phase resetting curves, and synchrony. *Neural Computation*, 8, 979-1001.
- Gerstner, W., van Hemmen, J.L., & Cowan, J.D. (1996). What matters in neuronal locking. *Neural Computation*, 8, 1653-1676.
- Gerstner, W., & Kistler, W. (2002). *Spiking neuron models*. Cambridge university press.
- Gutkin, B.S., & Ermentrout, G.B. (1998). Dynamics of membrane excitability determine interspike interval variability: a link between spike

generation mechanisms and cortical spike train statistics. *Neural Computation*, 10, 1047-1065.

Hansel, D., Mato, G., & Meunier, C. (1995). Synchrony in excitatory neural networks. *Neural Computation*, 7, 307-335.

Hodgkin, A.L. (1948). The local electric changes associated with repetitive action in a non-medullated axon. *J. Physiol. (Lond.)*, 107, 165-181.

Izhikevich, E.M. (2000). Neural excitability, spiking, and bursting. *Int. J. Bifurca. Chaos*, 10, 1171-1266.

Jolivet, R., Lewis, T., & Gerstner, W. (2004). Generalized integrate-and-fire models of neuronal activity approximate spike trains of a detailed model to a high degree of accuracy. *J. Neurophysiol.*, 92, 959-976.

Kistler, W.M., Gerstner, W., & van Hemmen, J.L. (1997). Reduction of the Hodgkin-Huxley equations to a single-variable threshold model. *Neural Computation*, 9, 1015-1045.

Koch, C., Bernander, Ö., and Douglas, R.J. (1995). Do neurons have a voltage or a current threshold for action potential initiation. *J. Comp. Neurosci.*, 2, 63-82.

Koch, C. (1999). *Biophysics of Computation*. Oxford University Press, New York.

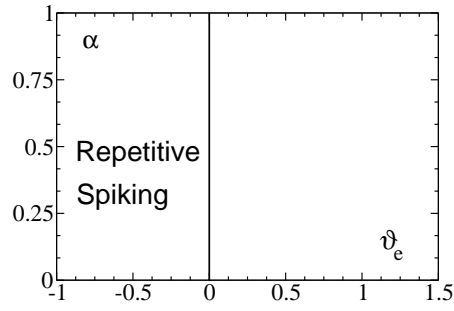
Noble, D., & Stein, R.B. (1966). The threshold conditions for initiation of action potentials by excitable cells. *J. Physiol.*, 187, 129-162.

Rinzel, J.M., & Ermentrout, G.B. (1998). Analysis of neuronal excitability. In C. Koch & I. Segev (Eds.), *Methods in Neuronal Modeling* (2nd ed.). Cambridge, MA:MIT Press.

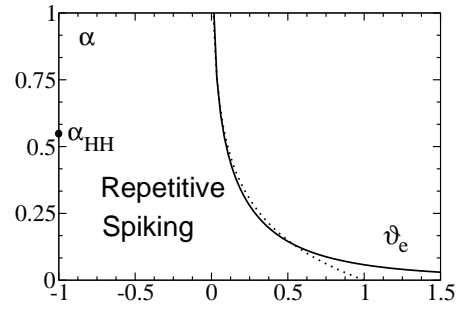
Tonnelier, A., & Gerstner, W. (2003). Piecewise linear differential equations and integrate-and-fire neurons: insights from two-dimensional membrane models. *Phys. Rev. E*, *67*, 021908.

Figure caption.

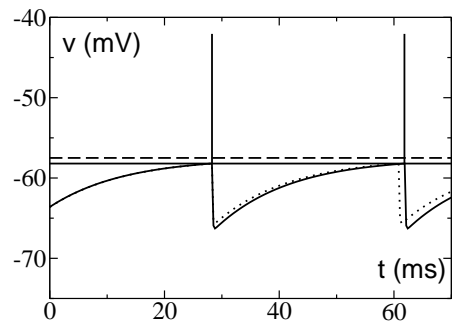
Figure 1. (A), (B) Locus of existence of periodic solutions obtained for (A) the type I and (B) the type II recovery kernel of the spike-response model in the (ϑ_e, α) plane. In (B), the dotted lines indicates if $-\eta_r(t)$ crosses the effective threshold (left part). Parameter α_{HH} is derived from Hodgkin-Huxley model (see below). Panels C and D show the periodic subthreshold potential of the spike-response model (solid lines) that approximates (C) the Connor *et al.* model and (D) the Hodgkin-Huxley model. The dotted lines represent the short term memory approximation. The neuron fires a spike (vertical line) when the voltage membrane hits the firing threshold (filled line). The stationary state (dashed line) is shown. Note that in panel (D), the model exhibits bistability between a stable steady state and stable oscillation. (E), (F) Action potential corresponding to (E, left) the Connor *et al* model; (F, right) the Morris-Lecar model; (F, left) the Hodgkin-Huxley model and (F, right) the FitzHugh-Nagumo model. These models have been stimulated by a short, but strong, current pulse before $t = 0$. A subthreshold DC current has also been applied. The horizontal line represents the stationary potential. Models of panel E are known as type I models whereas model of panel F are reported to as type II models. We idealize the spike (dotted lines) with a Dirac delta function and we fit (dashed lines) the recovery part with two generic kernels (see the text). The recovery part acts after a delay Δ . Numerical values are (E, left) $\mu_r = 17mV, \tau_r = 0.1985ms, \omega_r = 4.691MHz, \Delta = 9.5ms$, (E, right) $\mu_r = 40mV, \tau_r = 6, \omega_r = 0.1MHz, \Delta = 40ms$ and (F, left) $\mu_r = 28mV, \tau_r = 6ms, \omega_r = 0.3MHz, \Delta = 5ms$, (F, right) $\mu_r = 0.88, \tau_r = 12, \omega_r = 0.11, \Delta = 20.5$ (dimensionless units).



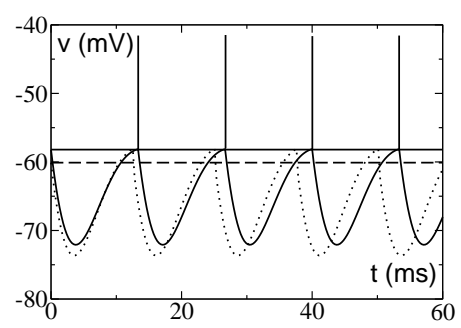
A



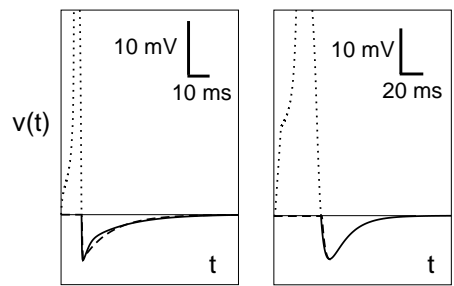
B



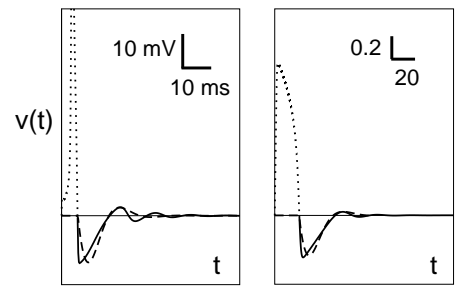
C



D



E



F